Monte Carlo Simulation of Radiation in Gases with a Narrow-Band Model and a Net-Exchange Formulation

CHERKAOUI Moha ($\diamond$), DUFRESNE Jean-Louis ($\diamond$), FOURNIER Richard ($\bullet, \oplus$), GRANDPEIX Jean-Yves ($\diamond, \bullet$), LAHELLEC Alain ($\diamond$)

($\diamond$) *Laboratoire de Météorologie Dynamique , C.N.R.S-Université Paris 6, F-75252 Paris Cedex 05, France*

($\bullet$) *LESETH, Université Paul Sabatier, F-31077 Toulouse Cedex, France*

($\oplus$) now at the *Institute of Energy and Power Plant Technology, TH Darmstadt, 64287 Darmstadt, Germany.*

published in ASME Journal of Heat Transfer, May 1996, pp.401-407

Abstract

The Monte Carlo method is used for simulation of radiative heat transfers in non-gray gases. The proposed procedure is based on a Net-Exchange Formulation (NEF). Such a formulation provides an efficient way of systematically fulfilling the reciprocity principle, which avoids some of the major problems usually associated with the Monte Carlo method : numerical efficiency becomes independent of optical thickness, strongly non uniform grid sizes can be used with no increase in computation times and configurations with small temperature differences can be addressed with very good accuracy. The Exchange Monte Carlo Method (EMCM) is detailed for a one-dimensional slab with diffusely or specularly reflecting surfaces.

I Introduction

While the role of infrared exchanges in gases is well known for very large (atmospheric) or very hot (combustion) systems, its importance in small, nearly isothermal systems at moderate temperature is much less advertised. And yet, several experimental investigations concerning natural convection in dwelling rooms using various configurations including highly reflective walls, seem to indicate a coupling between radiative processes and fluid flow (Yguel 1988, Palenzuela 1992, Fournier 1994). Thus, the present study was devoted to the development of a sufficiently precise method for radiation exchange computations within nearly isothermal cavities at moderate temperature, filled with an air / water vapor / carbon dioxide mixture, and having possibly reflecting walls.

Numerical simulations of radiative heat transfer in gases originated mainly in meteorology and astrophysics research (Goody and Yung, 1989) as well as in engineering heat transfer research for high temperature systems (Ludwig et al., 1973). Efforts concerned the development of gas radiation models and their implementation in complete radiation heat transfer simulations through the integration of the radiative transfer equation. Nowadays the use of "exact" line by line models remains unfeasible for complex systems ; most authors make use of accurate band models like the narrow band statistical model (NBSM) proposed by Malkmus in 1967. This type of model leads to specific difficulties, when solving the radiative transfer equation, due to spectral correlations, within each band, between intensity and gas transmittance. We will not enter in a detailed description of this phenomenon which is extensively discussed in the literature. The main points are :

i) whatever intrinsic precision band models may reach, final results can be very inaccurate if correlations are ignored,

ii) specific solutions have been proposed for black wall enclosures (for example Zhang et al., 1988) but the problem remains open when surface reflections occur (Menart et al., 1993a, Menart and Lee, 1993b).

One of the best available solution to this complex problem seems to be the use of the Monte Carlo method (MCM). Some care is required for emission/absorption correlations but solutions are available (Modest, 1992). For details about the use of the MCM with a NBSM one may also refer to Cherkaoui et al. (1992) and Liu and Tiwari (1993 and 1994). Two well advertised disadvantages of the MCM are the difficulty to cope with strongly non-uniform grids and the drastic increase of computation times with increasing optical thickness (Howell, 1988 and Siegel and Howell, 1992). A third difficulty appears, specific to nearly isothermal systems : radiation energy balances are very small compared to emitted and absorbed energies ; a one percent uncertainty on the computed absorbed and emitted energies may lead to more than a hundred percent error on the radiation balance of a given cell. Such configurations would demand extremely accurate computations, that is to say extremely large numbers of rays to follow, and hence prohibitive computer run times. Many efforts are being made in trying to improve the MCM : biasing techniques (Martin and Pomraning, 1990), reverse MCM (Walter and Buckius, 1992) and hybrid methods (Vercammen and Froment, 1980, Farmer and Howell, 1994). These different approaches represent good tools for specific problems but it can be a subtle task to choose among all available MCM improvements or to try to make use of several techniques simultaneously when required.

We started from the following statement : most of the aforementioned difficulties seem to be related to the violation of the reciprocity principle (this is particularly obvious for the problem of strong grid size differences). We therefore aimed at the development of a MCM that would intrinsically fulfill this principle. The approach used is entirely based on the concept of radiative exchange. The analogy to the physical processes is kept but emission and absorption mechanisms are considered simultaneously. In the standard MCM, when a ray between two points A and B is defined, it is used for the transport of energy from A to B. In the present method, the same ray will be used for the radiative *exchange* between A and B. This means that radiative transports from A to B and from B to A are not dissociated. This is achieved through the development of the net-

exchange formulation (NEF) described in Sec. II in the case of mono-dimensional configurations with black surfaces. Sec. III shows how the MCM can be efficiently applied on the basis of such a formulation. The extension to reflective surfaces and some validation tests are the subject of Sec. IV. Simulation results are presented in Sec. V.

II Net-Exchange Formulation (NEF)

The starting point is a formulation very similar to that proposed by Green (1967) for monochromatic radiative exchanges and extended by Joseph and Bursztyn (1976) for narrow band models. These authors were concerned with the simulation of radiative heat transfers in stratified planetary atmospheres. The present formulation has some common features with the zone formulation (Hottel, 1967), the main difference being that the assumption of isothermal cells is dropped.

(a) Monochromatic formulation. We consider here an infinite volume of gas at uniform pressure P confined between two parallel black plates. Plate 1 (at $S(1) = 0$ co-ordinate) is at temperature $\theta^s(1)$ and plate 2 ($S(2) = D$) is at temperature $\theta^s(2)$. As this configuration is one-dimensional we will only make use of fluxes and net fluxes per unit surface. The optical depth $\tau_\nu(x, x')$ between x and x' is defined as

$$\tau_\nu(x, x') = \left| \int_x^{x'} \frac{P_a(x'')}{P_0} \, k_\nu(x'') dx'' \right| \tag{1}$$

The net-exchange rate (NER) between two elementary gas layers at the x and x' co-ordinates is defined as the radiative flux emitted at x' and absorbed at x minus the radiative flux emitted at x and absorbed at x'. For a monochromatic radiation this NER can be written as (Green, 1967 ; Joseph and Bursztyn, 1976)

$$\frac{\partial^2 \psi_\nu^{gg}(x, x')}{\partial x \partial x'} = \pi [B_\nu(x') - B_\nu(x)] \left| \frac{\partial^2}{\partial x \partial x'} [\mathcal{T}_\nu(x, x')] \right| = -\frac{\partial^2 \psi_\nu^{gg}(x', x)}{\partial x' \partial x} \tag{2}$$

where $\mathcal{T}_\nu(x, x')$ is the monochromatic slab transmittance

$$\mathcal{T}_\nu(x, x') = 2 \int_0^1 \mu \exp(-\tau_\nu(x, x')/\mu) d\mu \tag{3}$$

Similar expressions can be derived for the NER between surface m and an elementary gas layer at x :

$$\frac{\partial \psi_\nu^{gs}(x, m)}{\partial x} = \pi \Big[B_\nu^s(m) - B_\nu(x) \Big] \left| \frac{\partial}{\partial x} \Big[\mathcal{T}_\nu\big(S(m), x\big) \Big] \right| = -\frac{\partial \psi_\nu^{sg}(m, x)}{\partial x} \tag{4}$$

and between the two surfaces

$$\psi_\nu^{ss}(1, 2) = \pi [B_\nu^s(2) - B_\nu^s(1)] \mathcal{T}_\nu\big(S(1), S(2)\big) = -\psi_\nu^{ss}(2, 1) \tag{5}$$

Local radiation balances may be expressed using partial exchanges. The resulting expression for the net inflow at x of monochromatic radiant energy per unit volume is :

$$\frac{\partial \psi_\nu^g(x)}{\partial x} = \int_0^D \frac{\partial^2 \psi_\nu^{gg}(x, x')}{\partial x \partial x'} dx' + \sum_{m=1}^{2} \frac{\partial \psi_\nu^{gs}(x, m)}{\partial x} \tag{6}$$

We shall use a term commonly used in the literature of atmospheric sciences : "radiation budget" is used instead of "radiation net flux" to avoid confusion between "net rates" and "net-exchange rates". Similarly the surface radiation budget at $S(1)$ is :

$$\psi_\nu^s(1) = \int_0^D \frac{\partial \psi_\nu^{sg}(1, x)}{\partial x} dx + \psi_\nu^{ss}(1, 2) \tag{7}$$

(b) Spectral integration. Preceding expressions can be integrated over a spectral interval of width $\Delta\nu$. If the interval is narrow enough, the black body intensity can be assumed uniform. Integration of Eq. (2) gives, for instance

$$\frac{\partial^2\overline{\psi}^{gg}(x,x')}{\partial x\partial x'} = \frac{1}{\Delta\nu}\int_{\Delta\nu}\frac{\partial^2\psi_\nu^{gg}(x,x')}{\partial x\partial x'}d\nu = \pi\Big[\overline{B}(x') - \overline{B}(x)\Big]\ \frac{1}{\Delta\nu}\left|\frac{\partial^2}{\partial x\partial x'}\Big[\int_{\Delta\nu}\mathcal{T}_\nu(x,x')d\nu\Big]\right| \quad (8)$$

Inverting the frequency and angular integration (see Eq. 3) leads to the following expression

$$\frac{\partial^2\overline{\psi}^{gg}(x,x')}{\partial x\partial x'} = \pi\Big[\overline{B}(x') - \overline{B}(x)\Big]\left|\frac{\partial^2\ \overline{\mathcal{T}}(x,x')}{\partial x\partial x'}\right| \quad (9)$$

with

$$\overline{\mathcal{T}}(x,x') = 2\int_0^1 \mu\ \overline{F}(x,x',\mu)d\mu \quad (10)$$

and

$$\overline{F}(x,x',\mu) = \frac{1}{\Delta\nu}\int_{\Delta\nu}\exp(-\tau_\nu(x,x')/\mu)d\nu \quad (11)$$

$\overline{\mathcal{T}}$ and $\overline{F}$ are respectively defined as the spectral average slab transmittance and the spectral average transmission function. Integration over the whole spectrum is obtained by adding the contributions of the N_b narrow bands :

$$\frac{\partial^2\psi^{gg}(x,x')}{\partial x\partial x'} = \sum_{l=1}^{N_b}\frac{\partial^2\overline{\psi}_l^{gg}(x,x')}{\partial x\partial x'}\Delta\nu_l \quad (12)$$

Averaging Eqs. (4) and (5) gives two very similar expressions for gas-surface and surface-surface exchanges. Up to this point, the only assumption made is the spectral independence of the black body intensity within a narrow band. It allows preserving the antisymmetry in (x,x') of the spectrally integrated NER. Various narrow band models may be used to approximate the average transmission function. Considering the initial application field of the present work (building thermal analysis) the Malkmus NBSM was retained with the assumption of uniform gas radiative properties

$$\overline{F}(x,x',\mu) = \overline{T}(u(x,x',\mu)) \quad (13)$$

where u is the effective path length and $\overline{T}$ is the Malkmus transmission function

$$u(x,x',\mu) = \left|\int_x^{x'}\frac{P_a(x'')}{P_0\ \mu}dx''\right| \quad (14)$$

$$\overline{T}(u) = \exp\Big\{-\Phi\Big[(1+2\overline{k}\ u/\Phi)^{1/2}-1\Big]\Big\} \quad (15)$$

(c) Discretization. The volume of gas is divided in N_d layers of thicknesses ΔX_i. We want to emphasize that the layers are not assumed isothermal ; the internal temperature profiles are accounted for, without restriction. If we consider the i^{th} gas layer, between the X_i and X_{i+1} abscissae, and the j^{th} gas layer, between X_j and X_{j+1}, Eq. (9) can be integrated in x and x' to give the average NER between layers i and j :

$$\overline{\psi}^{gg}(i,j) = \int_{X_i}^{X_{i+1}}dx\int_{X_j}^{X_{j+1}}dx'\ \frac{\partial^2\overline{\psi}^{gg}(x,x')}{\partial x\partial x'} = \int_{X_i}^{X_{i+1}}dx\int_{X_j}^{X_{j+1}}dx'\pi\Big[\overline{B}(x')-\overline{B}(x)\Big]\left|\frac{\partial^2}{\partial x\partial x'}\Big[\overline{\mathcal{T}}(x,x')\Big]\right| \quad (16)$$

Equivalent expressions can be derived for the NER $\overline{\psi}^{gs}(i,m)$ between layer i and surface m and $\overline{\psi}^{ss}(1,2)$ between surfaces 1 and 2. The average radiation budget for the i^{th} layer is :

$$\overline{\psi}^{g}(i) = \sum_{j=1}^{N_d}\overline{\psi}^{gg}(i,j) + \sum_{m=1}^{2}\overline{\psi}^{gs}(i,m) \quad (17)$$

and for surface 1, it is expressed as

$$\overline{\psi}^{s}(1) = \sum_{i=1}^{N_d} \overline{\psi}^{sg}(1,i) + \overline{\psi}^{ss}(1,2) \tag{18}$$

III The Monte Carlo Numerical Scheme

Radiative transfer specialists commonly refer to the MCM as a method for numerical simulation of a stochastic process : by invoking a probabilistic model of the radiative exchange process and also applying Monte Carlo sampling techniques, it is possible to choose a semi-macroscopic approach, and avoid many of the difficulties inherent in the averaging process of the usual integral equation formulations (Howell, 1968). The aforementioned probabilistic model is usually designed in strict analogy with the physical processes of photon emission, transmission and absorption : we will refer to such methods as Analogue Monte Carlo Methods (AMCM).

The present approach is significantly different. We make use of the MCM for numerical computation of multidimensional integrals (Press et al., 1992). No physical probabilistic model is required. An integral formulation is chosen (NEF) and a statistical method (MCM) is used to compute integrals. A major feature of such a method is that the sampling laws could be chosen arbitrarily and do not have to match any physical property.

(a) Principle. The Monte Carlo procedure for numerical estimation of an integral $\mathcal{A} = \int_{\mathcal{D}} f(\vec{v})\ d\vec{v}$ is the following

i) A probability density function $p(\vec{v})$ is chosen arbitrarily on $\mathcal{D}$ with the only constraint that it must be non zero on $\mathcal{D}$.

ii) The associated weighting function is defined as

$$w(\vec{v}) = f(\vec{v})/p(\vec{v}) \tag{19}$$

iii) N values of $\vec{v}$ are generated randomly according to $p(\vec{v})$ and for each value the corresponding weighting factor w is computed. The average value $< w >_N$ and variance $\sigma_N^2(w)$ of these N realizations of the variable $w(\vec{v})$ are then computed. $< w >_N$ and $\sigma_N^2(w)$ themselves are random variables.

iv) $\widetilde{\mathcal{A}} =< w >_N$ is an estimate of integral $\mathcal{A}$. The expectation of $\widetilde{\mathcal{A}}$ is $\mathcal{A}$. An estimate of the standard deviation of $\widetilde{\mathcal{A}}$ (henceforth named "statistical error") is $\widetilde{\sigma_N}(\widetilde{\mathcal{A}}) = N^{-0.5}\ \sigma_N(w)$

When computing sums instead of integrals, the preceding procedure is valid if replacing pdf's with discrete probabilities.

The key point of this method is the choice of probabilities and pdf. Again, this choice is a priori totally arbitrary. However an improper choice of probabilities may lead, for a prescribed precision, to an extremely large sampling size. Obviously, the criterion is the variance of $w(\vec{v})$. Thus one should choose $p(\vec{v})$ such that the variations of $f(\vec{v})/p(\vec{v})$ are minimal, keeping in mind that the random generation according to $p(\vec{v})$ must be feasible and computationally efficient. Probabilities may also be chosen to match physical properties (like the Lambert Law for surface emission angles). This may lead to an increase of computational costs but provides the developer with a useful physical insight into the numerical procedure.

(b) Probability functions. The MCM is applied to compute the multidimensional integrals that appear in the NEF. In this formulation, independent expressions correspond to the NER for each pair of cells. It is therefore natural (although not necessary) to preserve this independence in the numerical scheme. We detail hereafter the probability functions retained for the MCM integration of the NER between two gas layers.

The total NER between the i^{th} and the j^{th} gas layers is defined from Eqs. (9), (12) and (16) :

$$\psi^{gg}(i,j) = \sum_{l=1}^{N_b} \Delta\nu_l \int_{X_i}^{X_{i+1}} dx \int_{X_j}^{X_{j+1}} dx' \int_0^1 d\mu \quad f^{gg}(l,x,x',\mu) \tag{20}$$

with

$$f^{gg}(l,x,x',\mu) = \pi \left[\overline{B_l}(x') - \overline{B_l}(x)\right] 2\mu \quad \left| \frac{\partial^2}{\partial x \partial x'} \left[\overline{T}_l\big(u(x,x',\mu)\big)\right] \right| \tag{21}$$

Thus the total NER computation involves one discrete sum, one integral over angles and two integrals over the x and x' co-ordinates. According to the general procedure presented in the preceding paragraph we need to define probabilities for each of these quantities. The associated weighting function will then be (Eq.(19)) :

$$w_{ij}^{gg}(l,x,x',\mu) = \frac{f^{gg}(l,x,x',\mu)}{\mathcal{P}(l) p_i(x) p_j(x') q(\mu)} \tag{22}$$

Uniform densities are used for positions within layers i and j and the pdf of the direction cosine μ corresponds to an isotropic emission (Table 1).

In order to determine discrete probabilities for spectral bands, we tried to estimate roughly the NER $\overline{\psi}_l^{gg}(i,j)$ between i and j on each band l. This renders it possible to favor bands on which most of the radiative exchanges occur. If the pdf chosen for x, x' and μ are meaningful one can simply state that if $\tilde{x}$,$\tilde{x}'$ and $\tilde{\mu}$ are the average values of x, x' and μ according to $p_i(x)$, $p_j(x')$ and $q(\mu)$ respectively, then a rough estimate $\mathcal{X}_l^{gg}(i,j)$ of $\overline{\psi}_l^{gg}(i,j)$ is :

$$\mathcal{X}_l^{gg}(i,j) = \frac{f^{gg}(l,\tilde{x},\tilde{x}',\tilde{\mu})}{p_i(\tilde{x})\ p_j(\tilde{x}')\ q(\tilde{\mu})} \tag{23}$$

Therefore the following probability is chosen for the l^{th} spectral band :

$$\mathcal{P}(l) = \frac{|\mathcal{X}_l|}{\sum_{k=1}^{N_b} |\mathcal{X}_k|} \tag{24}$$

To avoid problems when $\theta(\tilde{x}) = \theta(\tilde{x}')$, the black body intensity differences that appears in Eq.(24) are replaced by their derivatives relative to temperature. Similar developments are required for gas-surface and surface-surface exchanges (Table 1).

It is worth mentioning that the distance traveled between emission and absorption points does not appear as a variable to be randomly generated. Two locations are generated independently within the two considered cells from which the "exchange distance" is simply computed.

(c) Implementation. The quantities to be numerically estimated are the NER for each pair of cells. The radiation budget of each cell is obtained by summing the NER between the considered cell and all other cells in the system (Eqs. (17,18)). The code (See Fig. 1) contains therefore $(N_d+2)(N_d+1)/2$ independent Monte Carlo computations - the NER between a cell and itself being zero per definition.

The estimation of each $\psi(i,j)$ requires the Monte Carlo computation of an n-dimensional integral : $n = 4$ in case of two gas layers ($\vec{v} = (x,x',\mu,l)$), $n = 3$ in case of a gas layer and a surface ($\vec{v} = (x,\mu,l)$) and $n = 2$ in case of two surfaces ($\vec{v} = (\mu,l)$). The algorithm, following strictly the scheme detailed in Sec. III(a), involves : i) random generation of N realizations of the vector $\vec{v}$ according to $p(x)$, $p(x')$, $q(\mu)$ and $\mathcal{P}(l)$ (see appendix), ii) computation of the weighting function $w(\vec{v})$ (Eqs. (19) and (22)), iii) storage of the sums of all w and w^2. Details are given in Fig. 1 for a two gas layer case.

Note that computing separately each NER allows specific optimization for each pair of cells. For instance, the statistical laws used for narrow-band sampling turn out to be quite different whether the two cells are geometrically far apart or nearly adjacent.

Many pseudo-random number generators may be used. As a matter of fact we did use five of them, from the very low grade RNDM (of the multiplicative congruential type) to the very high quality RANLUX ("subtract-with-borrow" algorithm modified according to Luscher (1994)), both implemented in the CERN program library (James, 1994). The results on which comparisons were made appeared compatible within statistical errors. This insensitivity is a strong argument for considering the present method as a good unbiased reference method.

IV One Dimensional Slab with Reflective Surfaces

It is well known that narrow band models become difficult to handle (because of correlation effects) as soon as multiple reflections can play a significant part in the total heat transfer. As mentioned above, the NEF is not affected by correlation effects, therefore the EMCM is quite efficient for such configurations. An outline of the method is presented in the case of gas-surface exchanges with specular reflections. A detailed account is given in a forthcoming technical note (Cherkaoui, 1996).

(a) Formulation. The NER between gas layer i and surface m in a narrow band l can be split into an infinite sum of NER via 0, 1, 2 ... r, ... reflections :

$$\overline{\psi}_l^{gs}(i,m) = \sum_{r=0}^{\infty} \overline{\psi}_l^{gs*}(i,m;r) \tag{25}$$

In the case of specular reflections, $\overline{\psi}^{gs*}$ can be written as

$$\overline{\psi}_l^{gs*}(i,m;r) = \int_{X_i}^{X_{i+1}} dx \int_0^1 d\mu \;\; h^{gs}\big(l,x,m,\mu,r\big) \tag{26}$$

with

$$h^{gs}\big(l,x,m,\mu,r\big) = \pi\ \epsilon_m \Big[\overline{B_l^s}(m) - \overline{B}(x)\Big]\ 2\ \mu\ R(r)\ \left|\frac{\partial}{\partial x}\Big[\overline{T}_l\big(U(r)\big)\Big]\right| \tag{27}$$

where $R(r)$ is the product of the r surface reflectivities and $U(r)$ is the total effective path length.

(b) Probability functions and implementation. The algorithm for the computation of radiative exchanges with reflecting surfaces is fairly similar to that presented in Section III for black surfaces. We again consider separately the NER for each pair of discretized elements. For a given pair we compute separately the NER without reflection and with more than one reflection. The term without reflection is computed with the algorithm presented for black surfaces; the only difference is that the surface emissivities need to be taken into account.

The term with more than one reflection is an infinite sum. Practically the reflections are considered one after the other as for a ray tracking technique and a truncation procedure is defined so that the computation is stopped as soon as further reflections do not participate significantly to the exchange. The overestimate ξ^{gs} of the truncation error after r_0 reflections is chosen such that

$$\xi^{gs}\big(l,x,m,\mu,r_0\big) \geq \left|\sum_{r=r_0+1}^{\infty} h^{gs}\big(l,x,m,\mu,r_0\big)\right| \tag{28}$$

Overestimation functions are proposed in (Cherkaoui, 1996). Probability functions are chosen as in the black body surfaces case, except for the narrow band probabilities: the NER rough estimate (Eq.23) is here replaced with

$$\mathcal{X}_l^{gs*}(i,m) = \frac{h^{gs}\big(l,\tilde{x},m,\tilde{\mu},1\big) + \xi^{gs}\big(l,\tilde{x},m,\tilde{\mu},1\big)}{p_i(\tilde{x})\ q(\tilde{\mu})} \tag{29}$$

which is the sum of the NER for one reflection and the truncation error overestimate for one reflection at $\mu = \tilde{\mu}$ and $x = \tilde{x}$. The resulting procedure is summarized hereafter :

i) x, μ and l are generated randomly according to $p(x)$, $q(\mu)$ and $\mathcal{P}(l)$ respectively.

ii) For each value of r, starting from $r = 1$, we compute the truncation error $\xi^{gs}(l, x, m, \mu, r)$ and we keep the first value r_0 for which $\xi^{gs}(l, x, m, \mu, r_0)$ is lower than the required precision.

iii) We then store the weighting factor w^{gs} associated with the first r_0 terms of h and the weighting factor W^{gs} associated with these first r_0 terms of h plus the truncation error :

$$w^{gs}_{im}(l, x, m, \mu, r_0) = \frac{\sum_{r=1}^{r_0} h^{gs}(l, x, m, \mu, r)}{\mathcal{P}(l)\ p_i(x)\ q(\mu)} \tag{30}$$

$$W^{gs}_{im}(l, x, m, \mu, r_0) = w^{gs}_{im}(l, x, m, \mu, r_0) + \frac{\xi^{gs}(l, \tilde{x}, m, \tilde{\mu}, r_0)}{\mathcal{P}(l)\ p_i(x)\ q(\mu)} \tag{31}$$

In this way the absolute value of the radiation budget ψ can be under and over-estimated by using the average weights $< w >$ and $< W >$:

$$|< w >| \leq |\psi| \leq |< W >| \tag{32}$$

For pure diffusive surfaces, the same probabilities can be used, the only difference in the procedure being that the direction μ is not kept constant along the path. At each reflection a new value of μ is generated according to the Lambert angular distribution. The path-length $U(r)$ takes these various angles into account.

(c) Validation tests. Most benchmark configurations for gas radiative transfer are in the high temperature field. Table 2 contains results of high precision EMCM simulations for configurations in which the gas is isothermal at $\theta = 1000K$ and is either pure carbon dioxide or pure water vapor at atmospheric pressure. In order to allow comparisons with published results, some simulations where held where only one spectral band is considered : the $3755cm^{-1}$ band for water vapor (extending from $2875cm^{-1}$ to $4250cm^{-1}$) and the $3715cm^{-1}$ band for carbon dioxide (extending from $3275cm^{-1}$ to $3875cm^{-1}$). Radiative band parameters are those published in Hartman et al. (1984), Soufiani et al. (1985), and Zhang et al. (1988). Our results are compatible (maximum 2% difference) with those published in Kim et al. (1991), Menart et al. (1993a and 1993b) and Liu and Tiwari (1994).

Various internal consistency tests were also performed. The first one consists simply in the simultaneous development and inter-comparison of two independent codes, one that corresponds exactly to the algorithm detailed in the present paper (Cherkaoui 93) and one that makes use of the same theoretical approach with a k-distribution method (Fournier 94). The second set of tests relates to the way reflections are handled. A double simulation is performed : one with two black surfaces, the other with a black surface facing a *specular* reflective surface (reflectivity ρ). It can be shown that, if the temperature is continuous at the gas/wall interface, the limit value of the volumetric radiation budget at the reflective wall is $1 + \rho$ times the radiation budget in the two black wall case. In the special case $\rho = 1$ that multiplication factor is equal to two as the gas sees the system twice, directly and through a "mirror" reflection. This property is verified within statistical errors in our computations. Finally, the numerical quality of the method was checked in numerous test runs with two highly reflective surfaces : over estimation of the truncation error is confirmed and convergence achieved without any noticeable bias even for several hundred reflections.

V Results

The EMCM has been used for analysis of a wide range of nearly isothermal configurations with specular as well as diffuse surfaces (Cherkaoui, 1993). Figures 2 and 3 are meant to illustrate the gain over AMCM.

1) *Computations are a few orders of magnitude faster and numerical efficiency is little dependent on the system optical thickness :* Figure 2 displays computation times for simulation of a one meter slab with black surfaces. The gas is at atmospheric pressure and consists of carbon dioxide mixed with a non absorbing gas composed of 79% nitrogen and 21% oxygen. The temperature profile is linear from the cold surface temperature ($\theta^s(1) = 295K$ at $S(1) = 0$) to the hot one ($\theta^s(2) = 305K$ at $S(2) = D = 1m$). EMCM computation times are compared with those required by the AMCM code previously detailed by Cherkaoui et al. with and without centering. In this centering technique, computed fluxes are offset by corresponding fluxes in the isothermal case (Cherkaoui et al., 1992). The numbers of bundles are tuned in order to obtain a 5% precision : typically several hundreds per cell pair. These results confirm those of Liu and Tiwari (1994) illustrating the fact that the MCM can be computationally efficient for the simulation of gas radiative heat transfer. The EMCM allows us to go further in two ways : computations are at least two orders of magnitude faster and the method remains operational for optically thick systems. Notice that the present approach accounts for non-uniform temperature profiles within each gas layer. Of course any further simplifying assumption (isothermal layers, uncorrelated reflections ...) would reduce the computational costs.

2) *Strongly non-uniform discretizations introduce no specific convergence difficulties :* Figure 3 displays volumetric radiation budgets in the pure carbon dioxide case with various surface emissivities. A strongly varied discretization is used in order to allow an accurate simulation of the large radiation budget gradients at the walls : 20 layers with sizes ranging from 5 mm to 10 cm and two zero thickness layers enabling the computation of the limit value of the radiation budget at the boundaries. These profiles are typical examples of convergence qualities that would not be achievable with a standard AMCM at acceptable computational costs.

Acknowledgments

We are grateful to Pr. J. Taine and A.Soufiani (EM2C laboratory, C.N.R.S. / E.C.P.) for valuable discussions all along this work and their providing us with Narrow Band Model databases. We would like to thank L. Fairhead for English editing and R. "Ribs" Franchisseur for proficient true-hacker support. This work was sponsored by PIRSEM/CNRS, ADEME "Service Habitat et Tertiaire" and "Ministère de la Recherche et de la Technologie".

Appendix : sampling procedures

The cumulative distributions of the statistical laws introduced in the present text can be inverted analytically. Therefore, sampling procedures can be derived on the basis of the simple relation :

$$A = g^{-1}(R) \tag{33}$$

where R is a random variable distributed uniformly in the unit interval and g is the cumulative distribution function of the random variable A to be sampled. We give hereafter the corresponding relations for abscissae (x or x') and direction cosine (μ). Sampling of x (Table 1) :

$$x = X_i + \Delta X_i \; R_x \tag{34}$$

Sampling of μ for isotropic angular distribution (Table 1) :

$$\mu = R_\mu \tag{35}$$

Sampling of μ for Lambert angular distribution :

$$\mu = \sqrt{R_\mu} \tag{36}$$

For the random generation of a spectral band according to the set of discrete probabilities $\mathcal{P}(1)$, $\mathcal{P}(2)$ ... $\mathcal{P}(N_b)$, R_l is generated uniformly in the unit interval and l is chosen as the solution of the following double inequality :

$$\sum_{k=1}^{l-1} \mathcal{P}(k) < R_l \leq \sum_{k=1}^{l} \mathcal{P}(k) \tag{37}$$

Bibliography

Cherkaoui, M., Dufresne, J. L., Fournier, R., Grandpeix, J. Y., Lahellec, A., and Palenzuela, D., 1992, "Two Procedures for Radiative Calculations with a Narrow-Band Statistical Model in a Volume of Gas at Room Temperature," *Proceedings of the 21st Eurotherm Seminar*, F. Allard, J. F. Sacadura, M. Spiga, eds., EETI Paris, pp. 123-131.

Cherkaoui, M., 1993, "Modelisation et Etude de Sensibilite des Echanges Radiatifs et Conductifs Couples dans une Cavité Remplie d'Air Ambiant," Ph.D. dissertation, Université Paris XII, Paris, France.

Cherkaoui, M., Dufresne, J. L., Fournier, R., Grandpeix, J. Y., Lahellec, A., 1996, "Net Exchange Formulation for one dimensional configurations with reflective surfaces" , *Technical Note submitted to ASME-JHT*

Farmer, J. T., Howell, J. R., 1994, "Monte Carlo Algorithm for Predicting Radiative Heat Transport in Optically Thick Participating Media," *Proceedings of the 10th International Heat Transfer Conference*, Vol. 2, G. F. Hewitt ed., pp. 37-42.

Farmer, J. T., Howell, J. R., 1994, "Hybrid Monte Carlo/Diffusion Methods for Enhanced Solution of Radiative Transfer in Optically Thick Nongray Media," ASME HTD - Vol. 276, pp. 203-212.

Fournier, R., 1994, "Rayonnement Thermique dans les Gaz : Analyse du Couplage avec la Convection Naturelle," Ph.D. dissertation, Université Paul Sabatier, Toulouse, France.

Goody, R. M., and Yung, Y. L., 1989, *Atmospheric Radiation*, Second edition, Oxford University Press.

Green, J. S. A., 1967, "Division of Radiative Streams into Internal Transfer and Cooling to Space," *Quarterly Journal of the Royal Meteorological Society*, Vol. 93, pp. 371-372.

Hartmann, J. M., Levi Di Leon, R., and Taine, J., 1984, "Line-by-Line and Narrow-Band Statistical Model Calculations for H_2O," *Journal of Quantitative Spectroscopy and Radiative Transfer*, Vol. 32, No. 2, pp. 119-127.

Hottel, H. C., and Sarofim, A. F., 1967, *Radiative Transfer*, McGraw-Hill, New York.

Howell, J. R., 1968, "Application of Monte Carlo to Heat Transfer Problems," *Advances in Heat Transfer*, Vol. 5, T. F. Irvine and J. P. Hartnett eds., pp. 1-54.

Howell, J. R., 1988, "Thermal Radiation in Participating Media : the Past, the Present and Some Possible Futures," ASME Journal of Heat Transfer, Vol. 110, pp. 1220-1229.

James, F., 1994, "RANLUX : A Fortran Implementation of the High-Quality Pseudorandom Number Generator of Luscher," *Computer Phys. Commun.*, Vol. 79, pp. 111-114.

Joseph, J. M., Bursztyn, R., 1976, "A Radiative Cooling Model in the Thermal Infrared for Application to Models of the General Circulation," *Journal of Applied Meteorology*, Vol. 15, pp. 319-325.

Kim, T. K., Menart, J. A., and Lee, H. S., 1991, "Nongray Radiative Gas Analyses using the S-N Discrete Ordinates Method," ASME Journal of Heat Transfer, Vol. 113, pp. 946-952.

Liu, J., and Tiwari, S. N., 1993, "Investigation of Two-Dimensional Radiation Using a Narrow Band Model and Monte Carlo Model," ASME HTD - Vol. 244, pp. 21-31.

Liu, J., and Tiwari, S. N., 1994, "Investigation of Radiative Transfer in Nongray Gases Using a Narrow Band Model and a Monte Carlo Simulation," ASME Journal of Heat Transfer, Vol. 116, pp. 160-166.

Ludwig, C. B., Malkmus, W., Reardon, J. E., and Thompson, J. A. L., 1973, "Handbook of Infrared Radiation from Combustion Gases," NASA SP-3080

Luscher, M., 1994, "A Portable High-Quality Random Number Generator for Lattice Field Theory Simulations," *Computer Phys. Commun.*, Vol. 79, pp. 100-110.

Malkmus, W., 1967, "Random Lorentz Band Model with Exponential-Tailed S-1 Line-Intensity Distribution Function," *Journal of the Optical Society of America*, Vol. 57, No. 3, pp. 323-329.

Martin, W. R., Pomraning, G. C., 1990, "Monte Carlo Analysis of the Backscattering of Radiation from a Sphere to a Plane," *Journal of Quantitative Spectroscopy and Radiative Transfer*, Vol. 43, No. 2, pp. 115-126.

Menart, J. A., Lee, H. S., Kim, T. K., 1993, "Discrete Ordinate Solutions of Nongray Radiative Transfer with Diffusely Reflecting Walls," ASME Journal of Heat Transfer, Vol. 115, pp. 184-193.

Menart, J. A., Lee, H. S., 1993, "Nongray Gas Analyses for Reflecting Walls Utilizing a Flux Technique," ASME Journal of Heat Transfer, Vol. 115, pp. 645-652.

Modest, M. F., 1992, "The Monte Carlo Method Applied to Gases with Spectral Line Structures," *Numerical Heat Transfer*, Part B, Vol. 22, pp. 273-284.

Palenzuela, D., 1992, "Instabilités des Ecoulements de Convection Naturelle en Cavité. Introduction a l'Etude des Couplages Convection-Rayonnement," Ph.D. dissertation, Université Paul Sabatier, Toulouse, France.

Press, W. H., Flannery, B. P., Teukolsky, S. A., and Vetterling, W. T., 1992, *Numerical Recipes*, Cambridge University Press, New York, USA.

Siegel, R., and Howell, J. R., 1992, *Thermal Radiation Heat Transfer*, McGraw-Hill, New York, Third edition.

Soufiani, A., Hartmann, J. M., and Taine, J., 1985, "Validity of Band-Model Calculations for CO_2 and H_2O Applied to Radiative Properties and Conductive-Radiative Transfer," *Journal of Quantitative Spectroscopy and Radiative Transfer*, Vol. 33, No. 3, pp. 243-257.

Vercammen, H. A. J., and Froment, G. F., 1980, "An Improved Zone Method Using Monte Carlo Techniques for the Simulation of Radiation in Industrial Furnaces," *International Journal of Heat and Mass Transfer*, Vol. 23, pp. 329-337.

Walters, D. V., and Buckius, R. O., 1992, "Rigorous Development for Radiation Heat Transfer in Nonhomogeneous Absorbing Emitting and Scattering Media," *International Journal of Heat and Mass Transfer*, Vol. 35, No. 12, pp. 3323-3333.

Yguel, F., 1988, "Etude de la Convection Naturelle Tridimensionnelle dans les Cavités Fermées de Grandes Dimensions," Ph.D. dissertation, Université de Poitiers , Poitiers, France.

Zhang, L., Soufiani, A., and Taine, J., 1988, "Spectral Correlated and Non-Correlated Radiative Transfer in a Finite Axisymmetric System Containing an Absorbing and Emitting Real Gas-Particle Mixture," *International Journal of Heat and Mass Transfer*, Vol. 31, No. 11, pp. 2261-2272.

Nomenclature

$\mathcal{A}$: integral to estimate

B : black body intensity , $W/(m^2.sr.cm^{-1})$; $B(x)$ is the black body intensity at temperature $\theta(x)$, and $B^s(m)$ is the black body intensity for the surface temperature $\theta^s(m)$

D : distance between the two surfaces, m

$\mathcal{D}$: integration spatial domain

$\overline{F}(\ )$: narrow band average transmission function

k_ν : monochromatic absorption coefficient, m^{-1}

$\overline{k}$: narrow band average absorption coefficient, m^{-1}

l : narrow band index

m : surface index

N : number of realizations

N_d : number of gas layers

N_b : number of narrow bands

$P_a(\ )$: partial pressure of the gas absorber

P_0 : standard pressure ($P_0 = 1$ atm)

$\mathcal{P}(\ )$: probability

$p(\ )$: abscissa probability density function

$q(\ )$: direction cosine probability density function

r : number of reflections

$S(\ )$: surface abscissa, m

$\overline{T}(\ )$: Malkmus transmission function

$\mathcal{T}$: slab transmittance

u : effective path length , m

w, W : statistical weights

x, x' : coordinate

X_i : abscissa of separation between gas layers $(i-1)$ and (i) , m

$\widehat{X}_i$: abscissa of layer (i) center, m

ΔX : gas layer thickness , m

$\Delta\nu$: wavenumber interval , cm^{-1}

ν : wavenumber , cm^{-1}

ϵ : surface emissivity

ρ : surface reflectivity

μ : cosine of cone angle (measured from normal of surface)

Φ : shape parameter for the Malkmus model

$\psi(i,j)$: energy net-exchange rate between (i) and (j), defined as the rate at which energy is emitted at (j) and absorbed at (i) minus the rate at which energy is emitted at (i) and absorbed at (j)

$\psi(i)$: radiation budget of layer (i) , W per unit of reference area, $W.m^{-2}$

θ : temperature, K

τ_ν : monochromatic optical depth , m

γ : optical path index

$\mathcal{X}_l$: rough estimate of $\overline{\psi}_l$

ξ : overestimate of the truncation error

$\sigma(\ )$: standard deviation

Superscripts :

$\overline{(\ )}_l$: average for narrow band l ; l index is omitted when irrelevant.

g : gas layers

gg : exchange between two gas layers

gs or sg : exchange between a gas layer and an opaque surface

s : opaque surface

ss : exchange between two opaque surfaces

$\tilde{}$: average according to the chosen pdf

Abbreviations :

AMCM : Analogue Monte Carlo Method

EMCM : Exchange Monte Carlo Method

MCM : Monte Carlo Method

NEF : Net-Exchange Formulation

NER : Net-Exchange Rate

pdf : probability density function

ψ	f	$p_i(x)$	$p_j(x')$	$q(\mu)$	$\mathcal{X}_l$
$\psi^{ss}(m,m')$	$f^{ss}(l,m,m',\mu) = \pi\left[\overline{B_l^s}(m') - \overline{B_l^s}(m)\right]\ 2\mu\ \overline{T}_l\big(u(S(m),S(m'),\mu)\big)$	$-$	$-$	2μ	$\dfrac{f^{ss}(l,m,m',\tilde{\mu})}{q(\tilde{\mu})}$
$\psi^{gs}(i,m)$	$f^{gs}(l,x,m,\mu) = \pi\left[\overline{B_l^s}(m) - \overline{B_l}(x)\right]\ 2\mu\ \left\lvert\dfrac{\partial}{\partial x}\left[\overline{T}_l\big(u(x,S(m),\mu)\big)\right]\right\rvert$	$\dfrac{1}{\Delta X_i}$	$-$	1	$\dfrac{f^{gs}(l,\tilde{x},m,\tilde{\mu})}{p_i(\tilde{x})\ q(\tilde{\mu})}$
$\psi^{gg}(i,j)$	$f^{gg}(l,x,x',\mu) = \pi\left[\overline{B_l}(x') - \overline{B_l}(x)\right]\ 2\mu\ \left\lvert\dfrac{\partial^2}{\partial x \partial x'}\left[\overline{T}_l\big(u(x,x',\mu)\big)\right]\right\rvert$	$\dfrac{1}{\Delta X_i}$	$\dfrac{1}{\Delta X_j}$	1	$\dfrac{f^{gg}(l,\tilde{x},\tilde{x}',\tilde{\mu})}{p_i(\tilde{x})\ p_j(\tilde{x}')\ q(\tilde{\mu})}$

Table 1: Function f to be integrated and chosen pdf for surface-surface, gas-surface and gas-gas radiation net exchanges with black surfaces.

Gaz	θ^s (K)	ϵ_1	ϵ_2	D (m)	$\psi^s(1)$ $(kW.m^{-2})$	$\psi^s(2)$ $(kW.m^{-2})$	volumetric radiative budget at center $(kW.m^{-3})$
H_2O	0.	1.	1.	1.	28.094 ± 0.015	–	-23.17 ± 0.04
				0.5	24.26 ± 0.01	–	-50.07 ± 0.07
				0.1	14.417 ± 0.005	–	-219.6 ± 0.4
		0.1	1.	0.5	2.425 ± 0.004	28.00 ± 0.01	-34.40 ± 0.06
H_2O	500.	0.5	0.5	1.	4.700 ± 0.004	–	-4.917 ± 0.012
				10^{-1}	2.473 ± 0.002	–	-43.08 ± 0.08
($3755cm^{-1}$				10^{-2}	0.6594 ± 0.0004	–	-130.0 ± 0.2
bande		0.1	0.1	1.	1.160 ± 0.002	–	-1.410 ± 0.005
only)				10^{-1}	0.7755 ± 0.0007	–	-14.08 ± 0.04
				10^{-2}	0.3448 ± 0.0003	–	-68.17 ± 0.15
CO_2	500.	0.5	0.5	1.	1.709 ± 0.002	–	-1.278 ± 0.004
				10^{-1}	1.094 ± 0.001	–	-18.05 ± 0.04
($3715cm^{-1}$				10^{-2}	0.3379 ± 0.0002	–	-66.09 ± 0.11
bande		0.1	0.1	1.	1.278 ± 0.004	–	-0.3395 ± 0.0018
only)				10^{-1}	18.05 ± 0.04	–	-5.175 ± 0.017
				10^{-2}	66.09 ± 0.11	–	-31.48 ± 0.08

Table 2: Surface radiation budget at the walls and volumetric radiation budget at center for high temperature configurations ($\theta^g = 1000K$, $\theta_1^s = \theta_2^s = \theta^s$)

Energy NER between surfaces

- computation of $\mathcal{X}_l^{ss}(1,2)$ for all the narrow-bands l
- M.C. computation of $\psi^{ss}(1,2)$ and its statistical error $\sigma(\psi^{ss}(1,2))$
- $\psi^{ss}(2,1) = -\psi^{ss}(1,2)$; $\sigma(\psi^{ss}(2,1)) = \sigma(\psi^{ss}(1,2))$

Energy NER between gaz layers and surfaces

- loop on $i = 1, N_d$
  - loop on $m = 1, 2$
    - computation of $\mathcal{X}_l^{gs}(i,m)$ for all the narrow-bands l
    - M.C. computation of $\psi^{gs}(i,m)$ and its statistical error $\sigma(\psi^{gs}(i,m))$
    - $\psi^{sg}(m,i) = -\psi^{gs}(i,m)$; $\sigma(\psi^{sg}(m,i)) = \sigma(\psi^{gs}(i,m))$
  - end loop
- end loop

Energy NER between gaz layers

- loop on $i = 1, N_d - 1$
  - loop on $j = i+1, N_d$
    - computation of $\mathcal{X}_l^{gg}(i,j)$ for all the narrow-bands l
    - M.C. computation of $\psi^{gg}(i,j)$ and its statistical error $\sigma(\psi^{gg}(i,j))$
    - $\psi^{gg}(j,i) = -\psi^{gg}(i,j)$; $\sigma(\psi^{gg}(j,i)) = \sigma(\psi^{gg}(i,j))$
  - end loop
- end loop

Radiative budgets

- loop on $m = 1, 2$
  - $\psi^{s}(m) = \sum_{m'=1}^{2} \psi^{ss}(m,m') + \sum_{i=1}^{N_d} \psi^{sg}(m,i)$
  - $\sigma(\psi^{s}(m))^2 = \sum_{m'=1}^{2} \sigma(\psi^{ss}(m,m'))^2 + \sum_{i=1}^{N_d} \sigma(\psi^{sg}(m,i))^2$
- end loop
- loop on $i = 1, N_d$
  - $\psi^{g}(i) = \sum_{m=1}^{2} \psi^{gs}(i,m) + \sum_{j=1}^{N_d} \psi^{gg}(i,j)$
  - $\sigma(\psi^{g}(i))^2 = \sum_{m=1}^{2} \sigma(\psi^{gs}(i,m))^2 + \sum_{j=1}^{N_d} \sigma(\psi^{gg}(i,j))^2$
- end loop

M.C. computation of $\psi^{gg}(i,j)$ and its statistical error $\sigma(\psi^{gg}(i,j))$

- $\psi^{gg}(i,j) = 0$; $\beta(i,j) = 0$
- loop on e=1,N "loop on the N realizations"
  - random generation of x, x', μ, l (see appendix)
  - computation of $w_{ij}(l, x, x', \mu,)$ (equation (22))
  - $\psi^{gg}(i,j) = \psi^{gg}(i,j) + \frac{1}{N}.w_{ij}$
  - $\beta(i,j) = \beta(i,j) + \frac{1}{N}.[w_{ij}]^2$
- end loop
- $\sigma(\psi^{gg}(i,j)) = \sqrt{\beta(i,j) - [\psi^{gg}(i,j)]^2}/\sqrt{N}$
- $\psi^{gg}(j,i) = -\psi^{gg}(i,j)$; $\sigma(\psi^{gg}(j,i)) = \sigma(\psi^{gg}(i,j))$

Figure 1: General EMCM algorithm and details for gas-gas NER computations.

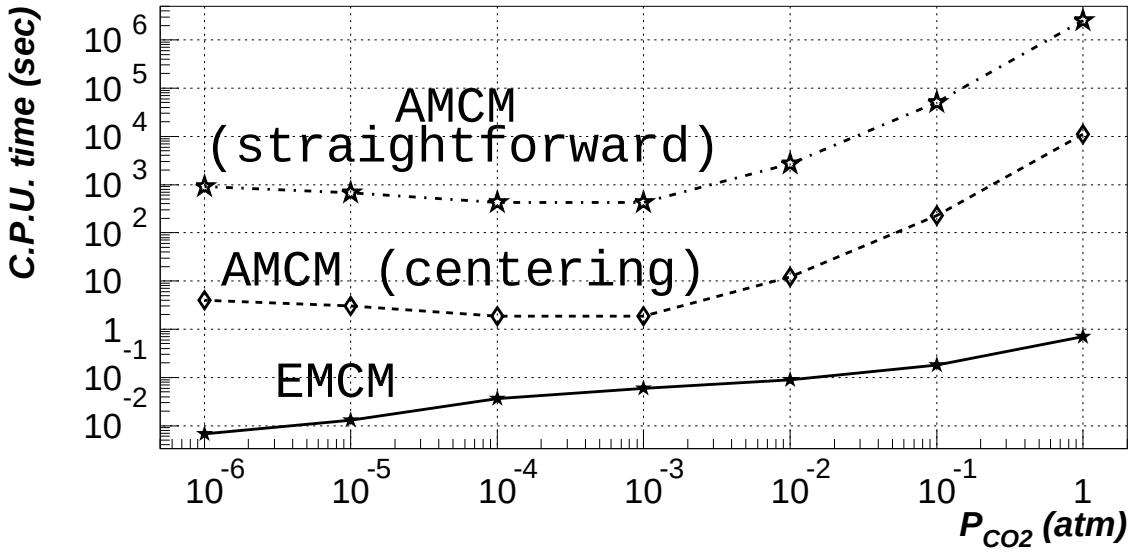

Figure 2: CPU time (with RNDM as random generator, on a 40 MFlops workstation HP-735) versus Carbon dioxide partial pressure for AMCM and EMCM. Bundles numbers are tuned to get a statistical error lower than 5% on radiation budgets 15cm off the surfaces. Both surfaces are black ($\epsilon_1 = \epsilon_2 = 1$) ; temperature profile is linear from $295K$ at $S(1) = 0$ to $305K$ at $S(2) = 1m$; the gas medium is regularly discretized into 10 layers.

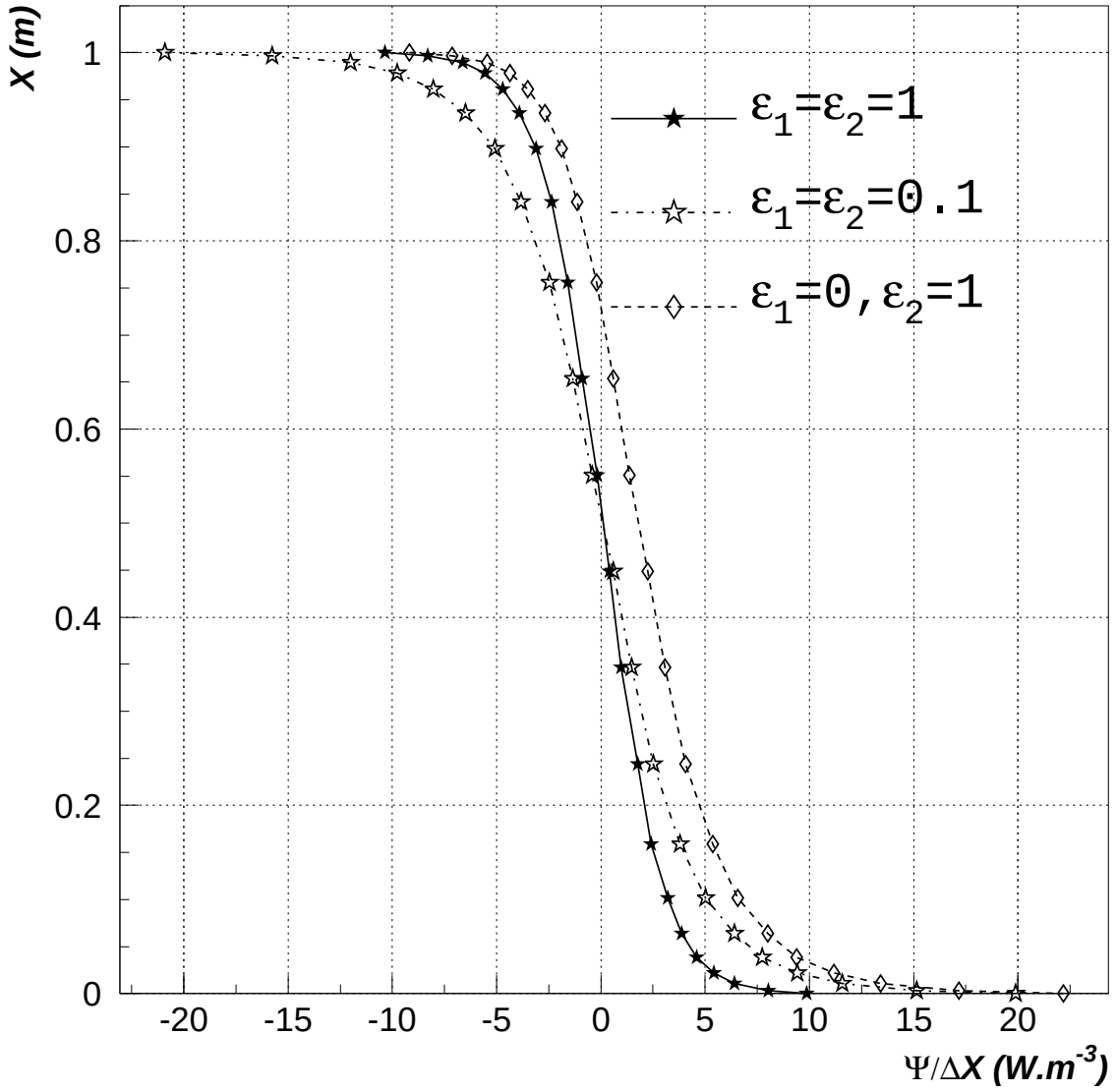

Figure 3: Volumetric radiation budget for pure CO_2 ($P_{CO_2} = 1atm$) with a linear temperature profile varying from $295K$ at $S(1) = 0$ to $305K$ at $S(2) = 1m$. The various diffuse surface emissivities are : $\epsilon_1 = \epsilon_2 = 1$; $\epsilon_1 = \epsilon_2 = 0.1$; $\epsilon_1 = 0, \epsilon_2 = 1$.